

## Order-disorder behavior in betaine arsenate studied by Raman scattering

Yu. I. Yuzyuk,\* J. Agostinho Moreira, A. Almeida, M. R. Chaves, and Filipa Pinto  
*Departamento de Física, IMAT (Núcleo IFIMUP), CFUP, Faculdade de Ciências da Universidade do Porto,  
 Rua do Campo Alegre, 687, 4169-007 Porto, Portugal*

A. Klöpperpieper  
*Fachbereich Physik, Universität des Saarlandes, D-66041 Saarbrücken, Germany*  
 (Received 6 July 1999)

A detailed study of Raman polarized spectra in betaine arsenate (BA) is presented. The results obtained give a significant contribution to the clarification of some controversial aspects of the critical behavior in BA. The temperature evolution of the hydrogen bonds stretching modes shows that different types of hydrogen bonds present different kinds of critical behavior. It also provides evidence of a proton ordering in the shorter hydrogen bond, i.e., along the  $c$  direction, at the para-ferroelectric phase transition. An order-disorder mechanism in the low-temperature region manifests itself by the progressive softening of the dynamical central peak observed in the low-frequency spectra. Furthermore, a hint of a short-range ordering below 150 K was found which is related to the existence of polar clusters even in the paraelectric phase.

### I. INTRODUCTION

Betaine arsenate,  $(\text{CH}_3)_3\text{NCH}_2\text{COO}\cdot\text{H}_3\text{AsO}_4$  (BA), undergoes two structural phase transitions: a ferrodistorptive ferroelastic phase transition at  $T_{c1}=411$  K and a ferroelectric phase transition at  $T_{c2}=119$  K. The spontaneous polarization appears in the  $ac$  plane, with the major component along the  $c$  axis.<sup>1</sup> It was assumed that BA is orthorhombic above  $T_{c1}$ , with the space group  $Pbnm^2$ . In the paraelectric-ferroelastic phase, the space group of BA is  $P12_1/n1$ .<sup>3</sup> Below  $T_{c2}$ , the space group  $P1n1$  was suggested.<sup>2</sup>

The order-disorder character of the phase transition in BA at  $T_{c2}$  was proposed from the high-frequency dielectric measurements, performed in the 0.1 MHz–10 GHz range,<sup>4</sup> where relaxation-type dispersion was observed. These data were analyzed assuming the occurrence of typical second-order ferroelectric phase transition and the value of  $\epsilon_o$  was found lower than the one reported by Klöpperpieper,<sup>1</sup> while  $\epsilon_\infty$  was unusually high. An additional relaxational soft mode at lower frequency (room-temperature value  $1/2\pi\tau=3$  cm<sup>-1</sup>) was revealed from submillimeter backwave oscillator response<sup>5</sup> but its temperature dependence was not reported. The analysis of submillimeter as well as microwave data obtained in solid solutions of BA and its deuterated analogs (BA-DBA) revealed two soft relaxational excitations polarized along the  $c$  axis<sup>4,5</sup> which is an important result. It was therefore proposed that lattice dynamics of BA-DBA solid solutions involves two temperature-dependent relaxational excitations and hence two subsystems of the ordered particles.<sup>5</sup>

Most of the experimental investigations of BA occasionally revealed some deviations from what is considered a typical ferroelectric behavior. Hysteresis loops in BA exhibit striking S-shaped curves in the temperature interval of 4 K above  $T_{c2}$  and in the temperature interval of 2 K below  $T_{c2}$ .<sup>6</sup> The onset of the saturation polarization occurs at  $T_{c2}-10$  K, approximately; at this temperature also an anomalous increase of the heat capacity was observed.<sup>7</sup> The pyroelectric coefficient along the  $c$  axis revealed two anomalies localized

in the temperature range 110–120 K.<sup>8</sup> The real part of the linear dielectric constant ( $\epsilon'$ ) showed a quasiplateau just below  $T_{c2}$ ; an additional anomaly of  $\epsilon'$  was observed at 4 K below  $T_{c2}$  at about the same temperature, where the pyroelectric current displayed a weak anomaly.<sup>8,9</sup> Very recently, two low-frequency strongly temperature-dependent relaxation modes were revealed from dielectric measurements in BA and its strongly deuterated analog DBA92 (degree of deuteration: 92%).<sup>10</sup> One of these modes, called the high-temperature mode (HT), was found in the whole temperature range studied, while the other one, the low-temperature mode (LT), was explicitly observed only below  $T_{c2}$  in BA and below 162 K in DBA92. The relaxation times of HT and LT modes exhibited sharp anomalies at 120 and 110 K, respectively. It was assumed that in BA the HT mode is related to antiferroelectric interactions and the LT mode is mainly related to ferroelectric ones.<sup>10</sup> New x-ray measurements put in evidence anomalies at 107 and 120 K and some precursor effects around 150 K in BA.<sup>11</sup> The phase transition sequence observed in BA-DBA system was discussed in the framework of a unique phenomenological model where two competing instabilities (ferroelectric and structural) were considered.<sup>12</sup> It was shown that BA-DBA represents a good example of a system where one of the order parameters suppresses the instability related to the other one. Experimental dielectric and acoustic data obtained for the samples with high degrees of deuteration (from 80 to 100%) were found in good agreement with the proposed phenomenological model.<sup>13</sup> Recently published results concerning Raman scattering in BA and DBA92 contributed to elucidate some aspects of the phase transitions in these compounds.<sup>14</sup> No soft mode was detected. The temperature behavior of the internal modes of the arsenate ions clearly shows important deformation of these units in both compounds. The existence of at least two types of hydrogen bonds was proposed and some evidence for the ordering of protons near  $T_{c2}$  in BA was found. This result was obtained by analyzing the temperature

dependence of the  $\nu_{2a}$  and  $\nu_{2b}$  fundamental internal modes of the arsenate ions.

Albeit the intensive studies performed in BA and its deuterated analog, our understanding of the basic interactions and of the microscopic mechanisms that lead to the ferroelectric phase transition are still far from being complete. Regarding the contribution of this work, particular attention is paid to both regions of external vibrations and stretching modes of the hydrogen bonds. The Raman study performed in the region of the O-H stretching modes is particularly interesting, as direct information regarding the phase transition can be obtained. A very detailed study of the behavior of the dynamical central peak provides a clear evidence of the existence of a relaxational mode. Thus an order-disorder character can be undoubtedly ascribed to the critical behavior of BA in the low-temperature region. A microscopic insight into the mechanisms underlying the ferroelectric phase transition in BA is given.

## II. EXPERIMENTAL PROCEDURE

The single crystal of BA used in this work has been grown from aqueous solution. The sample had the form of an oriented and optically polished rectangular parallelepiped of  $3 \times 4 \times 5$  mm<sup>3</sup>. As the monoclinic angle in BA is  $91.2^\circ$ , the sample was cut with faces normal to  $x \parallel a$ ,  $y \parallel b$  and  $z \parallel c$ , where  $a$ ,  $b$ , and  $c$  are the crystallographic monoclinic axes.

The polarized Raman spectra of BA have been measured in the right-angle scattering geometry. The 514.5 nm (300 mW) polarized light of an Ar<sup>+</sup> laser Coherent INOVA 90 was used for excitation. The scattered light was analyzed using a T64000 Jobin-Yvon spectrometer, equipped with a charge-coupled device and a photon-counting device. Identical conditions were maintained for all the scattering measurements. The spectral slit width was about  $1.5$  cm<sup>-1</sup>.

The sample was placed in a closed-cycle helium cryostat (10–300 K) with a temperature stability of  $\pm 0.2$  K. The temperature of the sample was estimated to differ by less than 1 K from the temperature measured with a silicon diode attached to the sample holder. The temperature homogeneity in the sample was achieved with a copper mask setup.

## III. RESULTS AND DISCUSSION

### A. External vibrations

According to x-ray data,<sup>3</sup> all atoms occupy sites of  $C_1$  symmetry in the paraelectric phase as well as in the ferroelectric one. The unit cell contains four formula units in both phases. The dynamics of the crystal lattice is described in terms of 321 optical and three acoustical phonons. As follows from factor group analysis, in the paraelectric phase one can expect 12  $A_g$  ( $xx$ ,  $yy$ ,  $zz$ ,  $xz$ ) and 12  $B_g$  ( $xy$ ,  $yz$ ) Raman lines in the low-frequency region corresponding to the translations and the librations of betaine molecules and of arsenate ions. In the ferroelectric phase, all modes become both infrared and Raman active and therefore  $22A'$  ( $xx$ ,  $yy$ ,  $zz$ ,  $xz$ ) and  $23A''$  ( $xy$ ,  $yz$ ) lines are allowed in the region of the external vibrations.

The low-frequency Raman spectra of such a complex crystal as BA with 108 atoms in the unit cell consist of strongly overlapped lines. Moreover, anharmonic large-

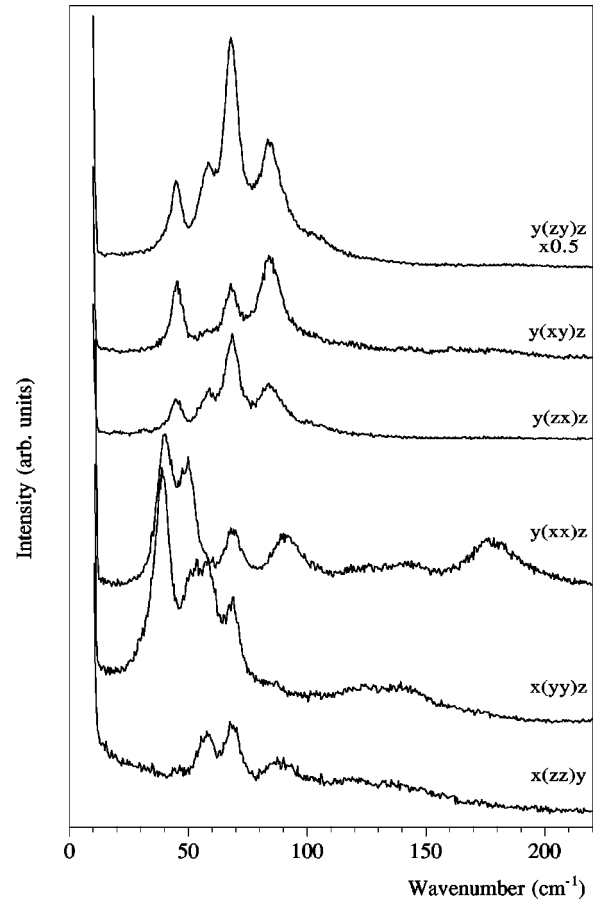


FIG. 1. The low-frequency Raman spectra of BA at room temperature for six scattering geometries.

amplitude reorientations of structural units in the unit cell have been evidenced in the room-temperature Raman spectra. These reorientations give rise to a dynamical central peak and lead to a significant broadening of the low-frequency spectra. However, by applying a fitting procedure it is possible to find all  $A_g$  and most of  $B_g$  external vibrations predicted by the factor group analysis. The Raman spectra of BA at room temperature for six scattering geometries are shown in Fig. 1 and the corresponding frequencies are listed in Table I.

The Raman spectra of BA (below  $230$  cm<sup>-1</sup>) were fitted with a sum of damped harmonic oscillators together with a Debye relaxator according to the general formula:

$$I(\omega, T) \approx [1 + n(\omega, T)] \left[ A_R \frac{\omega \tau_R}{1 + (\omega \tau_R)^2} + \sum_{j=1}^N A_{oj} \frac{\omega \Omega_{oj}^2 \Gamma_{oj}}{(\Omega_{oj}^2 - \omega^2)^2 + (\omega \Gamma_{oj})^2} \right]. \quad (1)$$

Here  $n(\omega, T)$  is the Bose-Einstein factor;  $A_{oj}$ ,  $\Omega_{oj}$ , and  $\Gamma_{oj}$  are the strength, frequency, and damping of the  $j$ th oscillator;  $A_R$  and the  $\tau_R$  are the strength and the relaxation time of the Debye relaxator, and  $N$  is the number of modes to fit. For the purpose of the fit, the Rayleigh scattering wing at the lowest frequencies was modeled by a fixed Gaussian component with a half width of about  $5$ – $6$  cm<sup>-1</sup> in the

TABLE I. Wave number (in  $\text{cm}^{-1}$ ) of the observed Raman bands for BA in the external mode region for the six scattering geometries at room temperature and at 40 K.

290 K ( $A_g$ )	40 K ( $A'$ )	290 K ( $B_g$ )	40 K ( $A''$ )
41	42		43
47	47	45	47
	51		51
59	57	59	54
	62		62
	70	68	69
70	75		76
			85
84	90	84	90
91	97		100
	101		
100	107	103	104
	112		111
	116		
123	122	120	121
	125		127
			137
142	146	141	145
156	156		155
	163	162	164
177	173		172
	179	178	181
	186		
192	204		200

whole temperature interval. The wing due to the integral contribution of the peaks at frequencies higher than  $230 \text{ cm}^{-1}$  were conveniently modeled by fixed Lorentzian components. The relaxator was included into the fitting procedure for spectra obtained in the  $yy$ ,  $zz$ , and  $zx$  orientations, while spectra in the  $xx$  and others nondiagonal orientations do not show any remarkable central peak.

The microscopic origin of this relaxator is suggested by the analysis of the Debye-Waller thermal factors of BA in the paraelectric phase. As was reported in Ref. 3 the largest value of the libration of the betaine molecule at room temperature have been observed around an axis parallel to the oxygen atoms of the carboxyl group. As show in Fig. 2, the C1, O1, and O2 atoms of the betaine molecule and the O3 and O5 oxygen atoms of the arsenate ion exhibit the largest

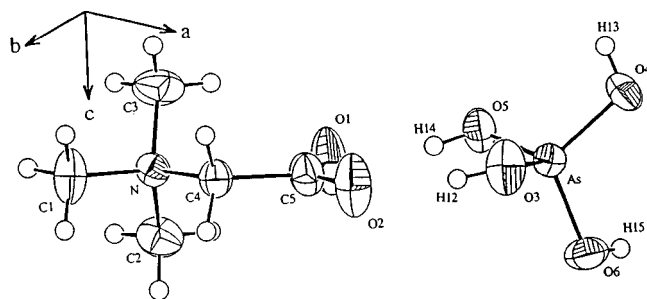


FIG. 2. ORTEP plot of the one unit formula of BA at room temperature.

amplitudes of thermal vibrations along the  $c$  axis. In turn, the O4 and O6 oxygen atoms of the arsenate ion have their largest amplitudes along the  $b$  axis. X-ray-diffraction method provides time-averaged information and the observed great anisotropy of thermal vibrations may be caused by anharmonic reorientations which give rise to a dynamical central peak, in the corresponding geometries in Raman scattering, namely,  $zz$  and  $yy$ .

The temperature evolution of the low-frequency Raman spectra is displayed in Fig. 3 and as can be seen from the results presented in Fig. 3(b), the relaxator exhibits progressive softening on cooling and its strength decreases considerably. Due to this process, low-frequency Raman lines become narrower and therefore better resolved below 200 K. Temperature dependence of the frequencies of the fitted Raman peaks and of the relaxator are shown in Figs. 4 and 5, respectively. As was mentioned above, the relaxation-type dispersion implying the order-disorder behavior in BA was previously observed at 1.6 GHz.<sup>4,10</sup> The temperature-dependent relaxator revealed in our Raman spectra below 1 THz, is obviously a different mode. Apparently, this high-frequency relaxation was previously observed by Goncharov *et al.*<sup>5</sup> at a somewhat lower frequency, although the temperature dependence of this mode was not referred in the publishing data as far as we know.

As the temperature is lowered toward  $T_{c2}$ , some modes which are active in the ferroelectric phase start to appear below 140–150 K. As a result, the number of lines at 123 K (just above  $T_{c2}$ ) is higher than expected from the factor group analysis. This behavior is an evidence of an intermediate regime characterized by a short-range order which starts to appear below 150 K, approximately. Due to the existence of this short-range order, polar clusters appear and infrared polar modes become active in Raman spectra. This behavior is typical of ill-ordered systems<sup>15</sup> and is consistent with a nonzero spontaneous polarization observed in BA far above  $T_{c2}$ .<sup>8,16</sup> Dielectric susceptibility and dielectric loss show a very important dispersion below  $T_{c2}$  in the low-frequency range,<sup>10</sup> also typical for disordered systems. Moreover, a nonlinear dielectric  $P$ - $E$  curve has been observed at  $T_{c2} + 4 \text{ K}$ .<sup>1</sup> This nonclosed S-shape hysteresis loop is also an evidence for an ill-ordered state.

The order parameter of this phase transition has a  $B_u$  symmetry and the soft relaxation mode should be infrared active in the paraelectric phase. The activation of this relaxator in  $A_g$  Raman species is obviously caused by the breaking of the selection rules, since large amplitude relaxations are not harmonic vibrations. As can be seen in Fig. 5, the reciprocal relaxation time  $\tau_R^{-1}$  fulfills the classical law for order-disorder ferroelectric phase transition:<sup>17</sup>  $\tau_R^{-1} = \gamma(T - T_c)$ . A linear least-squares-fit extrapolation of  $\tau_R^{-1}$  as a function of temperature yields  $T_c \approx (122 \pm 5) \text{ K}$ . Nevertheless, the central peak vanishes below 110 K. A narrow central mode centered at the laser line has been evidenced between 110 and 140 K. The width of this peak is of a few  $\text{cm}^{-1}$  and accurate parameters cannot be evaluated from Raman data due to the Rayleigh scattering. A likely explanation for this behavior is that a further critical narrowing of the central peak is effectively prevented by very low-frequency relaxations. These relaxations may arise from low-frequency cluster dynamics which vanish below 110 K.

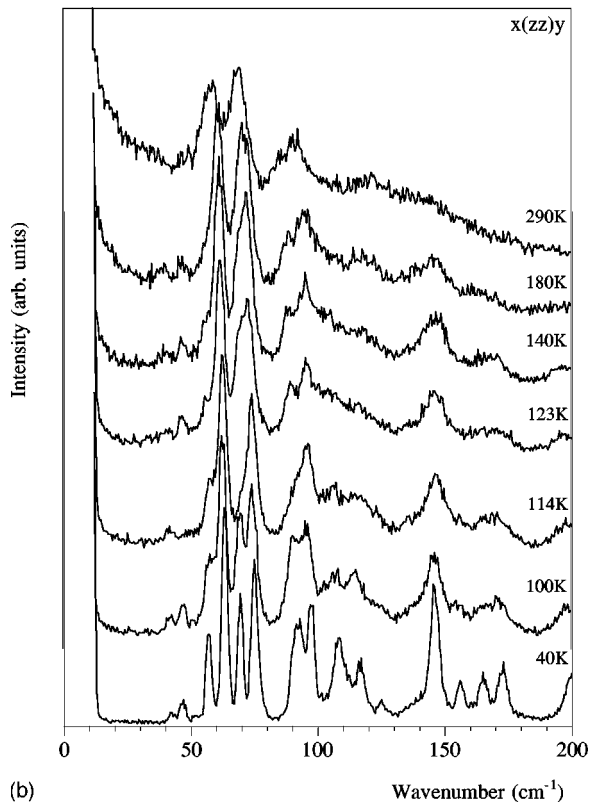
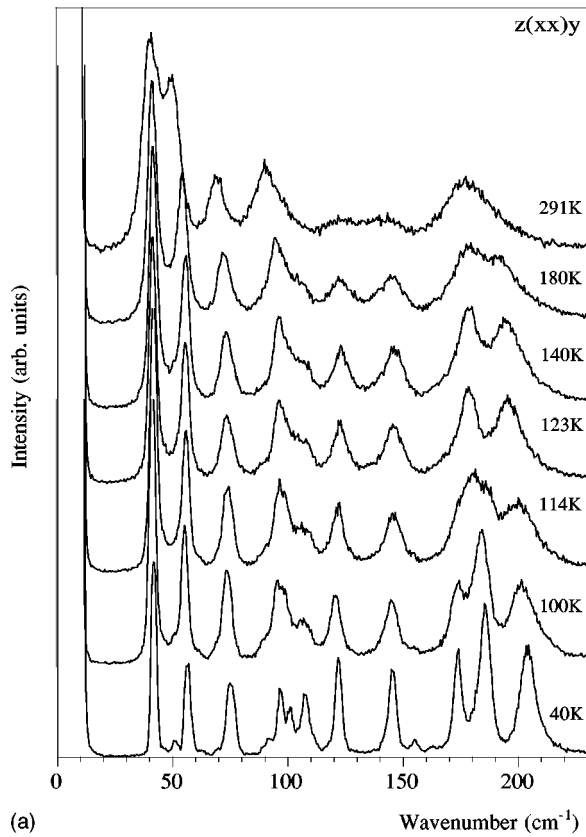


FIG. 3. The temperature evolution of the low-frequency Raman spectra for the  $z(xx)y$  (a) and for the  $x(zz)y$  (b) scattering geometries in BA.

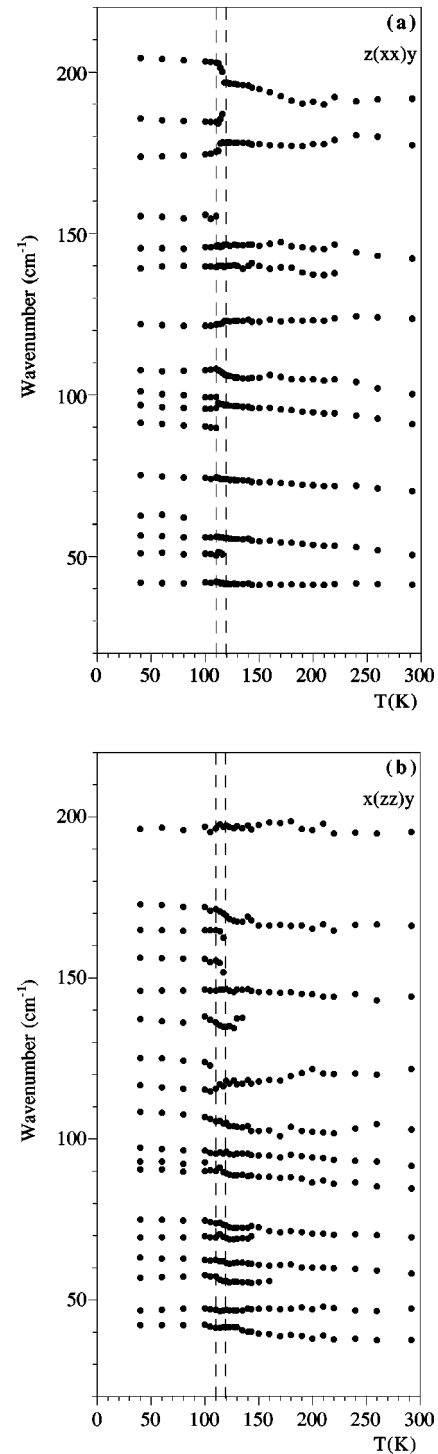


FIG. 4. The temperature dependences of the frequencies of the external modes in BA obtained from the fit of the  $z(xx)y$  (a) and from the  $x(zz)y$  (b) low-frequency Raman spectra.

As can be clearly seen in Fig. 4, most of the lines allowed in the ferroelectric phase only appear below 110 K. As a result the  $22A'$  and  $21A''$  Raman lines have been successfully observed (see Table I) in a good agreement with the factor group analysis, implying that the ferroelectric state is finally reached below 110 K. In the ferroelectric phase long-range electrostatic forces could result in a LO-TO splitting. As already known, the spontaneous polarization is very small in BA [ $10^{-3} \text{ cm}^{-2}$  (Refs. 8 and 10)] and consequently large

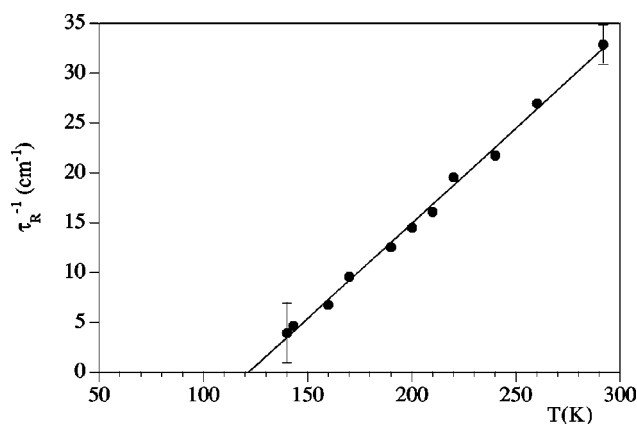


FIG. 5. The temperature dependence of the reciprocal relaxation time  $\tau_R^{-1}$  obtained from the fit. The solid line represents the best linear fit. Typical error bars at high and low temperatures are indicated.

LO-TO splittings are not expected. In fact, they have not been detected at all in our Raman spectra in the ferroelectric phase.

### B. Hydrogen bonds vibrations

It is now beyond any doubt that the low temperature phase transitions in BA, which is of order-disorder type, may be associated with the proton ordering and so it is interesting to know the temperature evolution of the Raman spectra in the frequency range corresponding to the hydrogen bonds modes.

The O–H $\cdots$ O lengths in BA have been found to be between 2.48 and 2.56 Å.<sup>3</sup> With such a bond length, the proton is situated in a double-well potential, as a rule. At room temperature, the Raman spectra of the stretching modes of H bonds in BA have shapes similar to the KDP-type crystals spectra with a dynamic distribution of protons between two potential minima on the O–H $\cdots$ O bonds. In the Raman spectra of BA, the two broad O–H $\cdots$ O stretching bands were observed at about 2900 and 2200  $\text{cm}^{-1}$  followed by a weak band at 1700  $\text{cm}^{-1}$ , labeled A, B and C, respectively, in Fig. 6. As shown in Fig. 6, the high-frequency A band is superimposed with numerous C–H stretching lines and therefore cannot be precisely studied. The line shape, intensity,

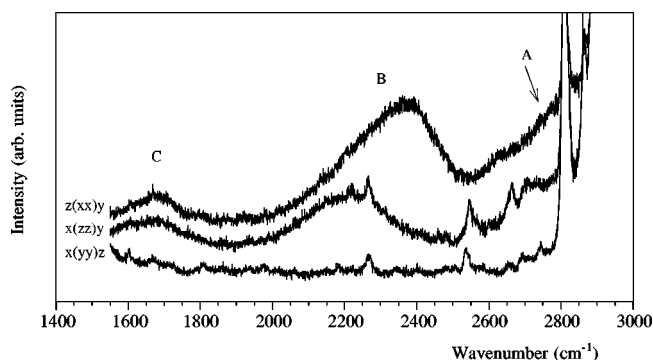


FIG. 6. The Raman spectra of BA in the diagonal scattering geometries at room temperature in the region of stretching vibrations of the hydrogen bonds.

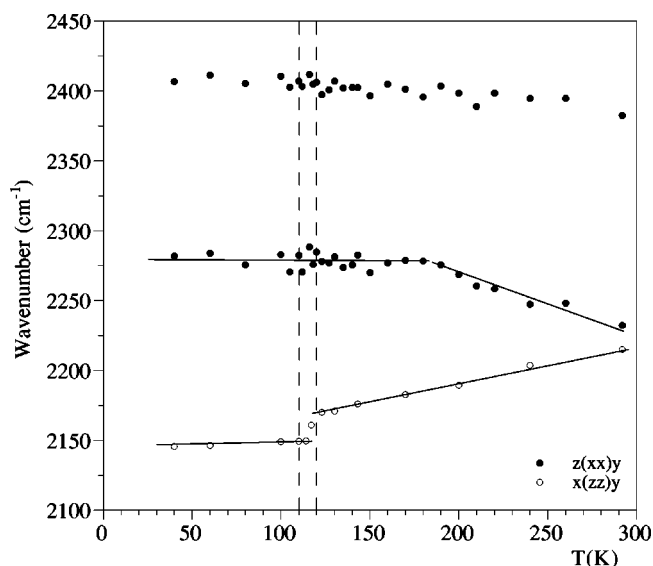


FIG. 7. The temperature dependence of the frequency of the B band obtained from the fit in the  $z(xx)y$  (full circles) and in the  $x(zz)y$  (open circles) scattering geometries. The solid lines are guides for the eyes.

and peak maximum of the B band exhibit large variations in distinct scattering geometries. Namely, no evidence of the stretching H-bond bands has been found in  $yy$  geometry. In  $zz$  geometry the B band is centered at 2215  $\text{cm}^{-1}$  while in  $xx$  geometry, the B band is strongly asymmetrical and consists of two bands centered at 2232 and 2382  $\text{cm}^{-1}$ . These peculiarities stem from the specific orientations of the H bonds in BA. As it was reported in Ref. 3, in the paraelectric phase, the  $\text{AsO}_4^{3-}$  ions are linked by H bonds forming a quasiunidimensional zigzag chain along the  $c$  axis in the unit cell. As can be seen in Fig. 2, one of these bonds (O4–H13 $\cdots$ O4) is mainly oriented along the  $c$  axis, while the other one (O6–H15 $\cdots$ O6) is mainly along the  $a$  axis. The betaine molecule is linked to the arsenate ion via two hydrogen bonds which are mainly oriented along the  $a$ -axis.

As it is known, the intensities of stretching H-bond bands show directional behavior in the Raman spectra. The highest intensities are observed when the electric field of both incident and scattered radiation are oriented parallel to the H-bond direction. Therefore, in case of BA, the B band centered at 2215  $\text{cm}^{-1}$  in  $zz$  geometry obviously originates from the shorter H bond O4–H13 $\cdots$ O4 (2.48 Å). The asymmetrical B band in  $xx$  geometry is thus attributed to the stretching vibrations of the remaining H bonds, oriented along the  $a$  axis.

The temperature dependences of the wave number of the B bands are presented in Fig. 7. The asymmetrical B band in  $xx$  spectra was fitted by a sum of two damped oscillators. Both components in the  $xx$  geometry do not exhibit anomalies at 120 or 110 K. However, it is noticeable that the low-frequency B band at 2232  $\text{cm}^{-1}$  (value at room temperature) shows hardening as the temperature is lowered from 291 to 180–190 K albeit no variation has been observed on further cooling. The frequency of the second B band at 2382  $\text{cm}^{-1}$  (value at room temperature) remains practically unchanged in the whole temperature range, implying that the bond

length does not change with temperature variation. In contrast, a progressive decreasing of the peak maximum has been observed on cooling for the B band in  $zz$  geometry. Furthermore, a very clearly defined drop has been detected at  $T_{c2}$ . This downward shift of the peak maximum is a direct evidence of the strengthening of the H bond below  $T_{c2}$ .<sup>18,19</sup> Thus one can conclude that spontaneous polarization along the  $c$  direction starts to appear due to the proton ordering in the shorter O4–H13···O4 hydrogen bond.

#### IV. CONCLUSIONS

These Raman-scattering experiments allow the detailed outlining of some important features of the lattice dynamics of BA and which are stated in the following. In the region of external vibrations, the experimental Raman spectra are in good agreement with factor group analysis in both paraelectric-ferroelastic and ferroelectric phases. An evidence of a short-range ordering occurring below 150 K was found from the analysis of the temperature evolution of the low-frequency Raman spectra for different scattering geometries.

A dynamical central peak of appreciable intensity and width was observed in the Raman spectra and it was well fitted by a Debye relaxator, whose progressive softening is a direct evidence of an order-disorder phase transition mechanism. The microscopic origin of the relaxation was attributed to the reorientations of the betaine-arsenate units.

In an early paper on BA,  $T_{c2} = 119$  K was referred as the para-ferroelectric phase transition temperature,<sup>1</sup> but afterwards some anomalies below and above  $T_{c2}$  were revealed with different techniques.<sup>8–11</sup> Some features similar to a glasslike behavior have been disclosed in this pure compound and a transition to a mixed ferroelectric-glass phase was proposed.<sup>8</sup> This unusual behavior in a pure compound is due to the existence of antiferroelectric and ferroelectric competitive interactions which have their origin in some peculiarities of the crystal structure of BA.

All protons are distributed among fourfold positions of  $C_1$  symmetry in the unit cell and thus three kinds of symmetrically nonequivalent hydrogen bonds exist. As follows from

the analysis of our Raman measurements, the hydrogen bonds oriented along the  $c$  axis and the  $a$  axis exhibit quite different behavior on cooling and their ordering likely occurs at different temperatures. The ordering of protons in the hydrogen bonds along the  $c$  axis occurs at 120 K and coincides with the sharp anomalies of pyroelectric current and dielectric amplitude of the HT mode. Although the temperature of the ordering of protons along the  $a$  axis is not clear in our results, infrared spectroscopy provides a strong evidence of the proton ordering in that direction near 110 K,<sup>20</sup> where the additional anomaly of pyroelectric current and the sharp anomaly of the dielectric amplitude of the LT mode were observed.<sup>10</sup> The spontaneous polarization progressively increases and different external Raman lines, which are expected in the polar phase, appear below 100 K. Thus, a ferroelectric state is finally reached as the structure is ordered both in  $a$  and in  $c$  directions. Between 120 and 110 K BA is therefore an ill-ordered system. This conclusion is consistent with previously reported dielectric dispersion data obtained in a narrow temperature interval below 120 K.<sup>8</sup>

BA has thus proven to be an interesting example of a nominally pure compound where competitive interactions in the hydrogen bond network together with reorientations of betaines molecules and arsenate ions lead to numerous effects which are typical of ill-ordered systems. And, as we have shown, Raman-scattering results provide a microscopic insight into the nature of the competing instabilities in BA.

#### ACKNOWLEDGMENTS

The authors gratefully thank Professor R. Pick for enlightening discussions and Dr. J. Albers for his collaboration in the study of betaine compounds. The authors thank A. Costa for his technical assistance. This work was supported by Fundação para a Ciência e para a Tecnologia (FCT) Project No. PRAXIS/2/2.1/FIS/26/94. Yu. I. Yuzyuk, J. Agostinho Moreira, and Filipa Pinto thank Projecto Praxis XXI for their grants: Nos. BCC/17125/98, BD/3192/94, and BICJ/4688/96, respectively.

\*On leave from the Faculty of Physics, Rostov State University, Rostov-on-Don, Russia.

<sup>1</sup>A. Klöpperpieper, H. J. Rother, J. Albers, and K. H. Ehses, *Ferroelectr. Lett. Sect.* **44**, 115 (1982).

<sup>2</sup>S. Hayase, T. Koshihara, H. Terauchi, M. Maeda, and I. Suzuki, *Ferroelectrics* **96**, 221 (1989).

<sup>3</sup>W. Schildkamp, G. Schäfer, and J. Spilker, *Z. Kristallogr.* **168**, 187 (1984).

<sup>4</sup>O. Freitag, H. J. Brückner, and H.-G. Unruh, *Z. Phys. B: Condens. Matter* **61**, 75 (1985).

<sup>5</sup>Yu. G. Goncharov, G. V. Kozlov, A. A. Volkov, J. Albers, and J. Petzelt, *Ferroelectrics* **80**, 221 (1988).

<sup>6</sup>H. E. Müser and U. Schell, *Ferroelectrics* **55**, 279 (1984).

<sup>7</sup>K. -P. Frühauf, E. Sauerland, J. Helwig, and H. E. Müser, *Ferroelectrics* **54**, 293 (1984).

<sup>8</sup>A. Almeida, P. Carvalho, M. R. Chaves, and J. C. Azevedo, *Ferroelectr. Lett. Sect.* **9**, 107 (1988).

<sup>9</sup>M. T. Lacerda-Aroso, J. L. Ribeiro, M. R. Chaves, A. Almeida,

L. G. Vieira, A. Klöpperpieper, and J. Albers, *Phys. Status Solidi B* **185**, 265 (1994).

<sup>10</sup>A. Almeida, J. Agostinho Moreira, M. R. Chaves, A. Klöpperpieper, and Filipa Pinto, *J. Phys.: Condens. Matter* **10**, 3035 (1998).

<sup>11</sup>J. Agostinho Moreira, J. M. Kiat, A. Almeida, M. R. Chaves, and A. Klöpperpieper, *Phys. Status Solidi A* **178**, (2000).

<sup>12</sup>E. V. Balashova and A. K. Tagantsev, *Phys. Rev. B* **48**, 9979 (1993).

<sup>13</sup>E. V. Balashova, V. V. Lemanov, A. K. Tagantsev, A. B. Sherman, and Sh. H. Shomuradov, *Phys. Rev. B* **51**, 8747 (1995).

<sup>14</sup>J. Agostinho Moreira, A. Almeida, M. R. Chaves, M. F. Mota, A. Klöpperpieper, and Filipa Pinto, *J. Phys.: Condens. Matter* **10**, 6825 (1998).

<sup>15</sup>J. Petzelt, S. Kamba, and I. Gregora, *Phase Transit.* **63**, 107 (1997).

<sup>16</sup>J. Agostinho Moreira, L. C. R. Andrade, M. M. R. Costa, A. Almeida, M. R. Chaves, and A. Klöpperpieper, *Phys. Status Solidi A* **171**, 417 (1999).

- <sup>17</sup>J. Petzelt, G. V. Kozlov, and A. A. Volkov, *Ferroelectrics* **73**, 101 (1987).
- <sup>18</sup>A. Almeida, P. Simeão Carvalho, M. R. Chaves, A. Klöpperpieper, and J. Albers, *Phys. Status Solidi B* **184**, 225 (1994).

- <sup>19</sup>A. Novak, *Struct. Bonding (Berlin)* **18**, 117 (1974).
- <sup>20</sup>J. Agostinho Moreira, M. L. Santos, M. R. Chaves, A. Almeida, A. Klöpperpieper, and F. Gervais *Ferroelectrics* (to be published).